

Furoxans (1,2,5-Oxadiazole-*N*-Oxides) as Novel NO Mimetic Neuroprotective and Procognitive Agents

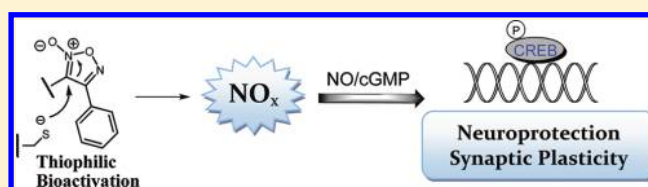
Isaac T. Schiefer,[†] Lawren VandeVrede,[†] Mauro Fa',[‡] Ottavio Arancio,[‡] and Gregory R. J. Thatcher^{*†}

[†]Department of Medicinal Chemistry and Pharmacognosy, College of Pharmacy, University of Illinois at Chicago, (MC 781), 833 South Wood Street, Chicago, Illinois 60612-7231, United States

[‡]Department of Pathology, The Taub Institute for Research on Alzheimer's Disease and the Aging Brain, Columbia University, P&S 12-420D, 630 West 168th Street, New York, New York 10032, United States

S Supporting Information

ABSTRACT: Furoxans (1,2,5-oxadiazole-*N*-oxides) are thiol-bioactivated NO-mimetics that have not hitherto been studied in the CNS. Incorporation of varied substituents adjacent to the furoxan ring system led to modulation of reactivity toward bioactivation, studied by HPLC-MS/MS analysis of reaction products. Attenuated reactivity unmasked the cytoprotective actions of NO in contrast to the cytotoxic actions of higher NO fluxes reported previously for furoxans. Neuroprotection was observed in primary neuronal cell cultures following oxygen glucose deprivation (OGD). Neuroprotective activity was observed to correlate with thiol-dependent bioactivation to produce NO₂⁻, but not with depletion of free thiol itself. Neuroprotection was abrogated upon cotreatment with a sGC inhibitor, ODQ, thus supporting activation of the NO/sGC/CREB signaling cascade by furoxans. Long-term potentiation (LTP), essential for learning and memory, has been shown to be potentiated by NO signaling, therefore, a peptidomimetic furoxan was tested in hippocampal slices treated with oligomeric amyloid- β peptide ($A\beta$) and was shown to restore synaptic function. The novel observation of furoxan activity of potential therapeutic use in the CNS warrants further studies.



■ INTRODUCTION

The wide range of biological activity of compounds containing a furoxan (1,2,5-oxadiazole-*N*-oxide) or benzofuroxan heterocycle has been known for decades.^{1–3} Although thermally stable and stable toward a range of acid–base conditions, furoxans are thiophilic electrophiles.⁴ This reactivity may underlie observed biological activity; for example, nitrobenzofuroxans were described as “thiol-neutralizing agents” in early work on the antileukemic properties of benzofuroxans and benzofurazans.^{5,6} However, the most commonly accepted mechanism underlying furoxan activity involves thiol-dependent NO release.⁷ In recent years, the furoxan moiety has been the subject of increased attention, pioneered by Gasco and others, owing to a plethora of interesting biological activities observed against a diverse range of targets.^{8–19} The majority of these efforts have focused on highly reactive furoxans that produce large fluxes of NO, thereby eliciting the cytotoxic effects associated with NO at high concentrations. Indeed, while NO possesses cytotoxic effects at high concentrations, low levels of NO are potentially protective, particularly in the CNS.²⁰ Despite ample attempts to develop furoxans as NO mimetics, efforts have not been directed at the potential for neuroprotection in the CNS. While the furoxan ring possesses inherent reactivity toward thiols, the identity and pattern of furoxan substitution can potentially dictate reactivity and the propensity for NO release, and therefore may be manipulated to produce furoxans with attenuated reactivity, which may hold potential as neuroprotective agents.

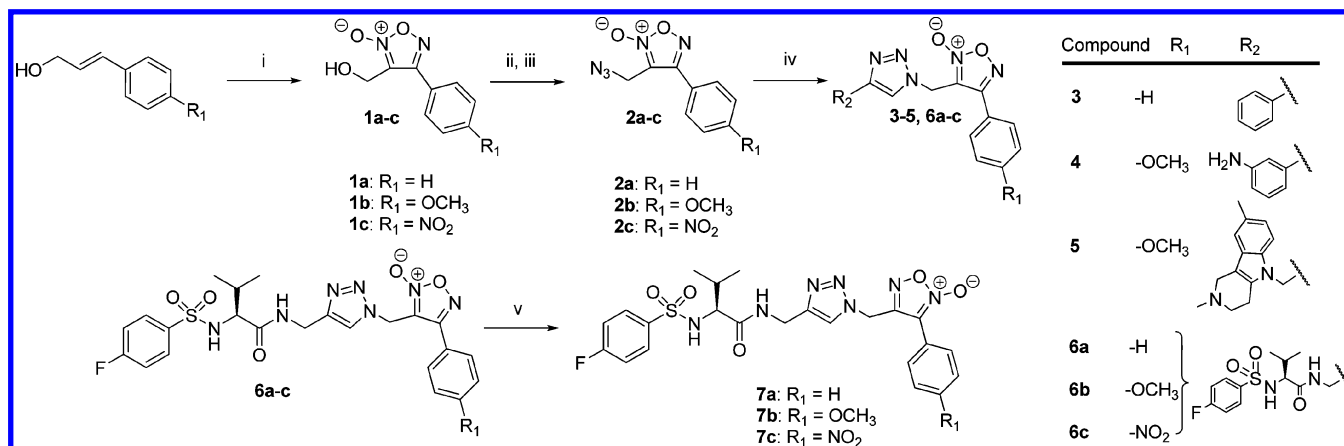
NO signaling via the second messenger molecule, cGMP, is essential for normal brain function.²¹ NO stimulates cGMP production through the activation of NO-sensitive soluble guanylyl cyclase (sGC or NO-GC), which in turn leads to activation of the memory-related transcription factor, cyclic-AMP response element binding protein (CREB).^{22–25} Moreover, evidence indicates that NO may act directly in presynaptic neurons.²⁶ At physiological concentrations, NO possesses a variety of neuroprotective and procognitive effects via a combination of cGMP-dependent and independent pathways, the latter proposed to include *S*-nitrosation of the active site cysteine of caspase-3 inhibiting execution of apoptotic cell death.²⁷

Enhancement of NO/sGC signaling may provide a novel approach to the treatment of Alzheimer's disease (AD) and other neurodegenerative disorders through neuroprotective and procognitive actions.^{20,28–32} Brain derived neurotrophic growth factor (BDNF), a downstream target of CREB, nourishes neurons, resulting in increased neurogenesis and enhanced synaptic plasticity.^{33–35} BDNF impairment has been demonstrated in the AD brain, and $A\beta$, the major component of amyloid plaques, has been shown to inhibit NO/sGC/CREB signaling, leading to synaptic impairment.³⁶ The importance of NO signaling in modulating synaptic plasticity and its correlation to enhanced learning and memory, as well as the

Received: November 7, 2011

Published: March 19, 2012

Scheme 1

Scheme 2^a

^aReagents and conditions: (i) NaNO₂, acetic acid, <20 °C; (ii) TsCl, TEA, CH₂Cl₂, 0 °C; (iii) NaN₃, DMF, 60 °C; (iv) CuI, DIPEA, toluene, with phenylacetylene for 3, 2,8-dimethyl-5-(prop-2-ynyl)-2,3,4,5-tetrahydro-1H-pyrido[4,3-b]indole for 5, (S)-2-(4-fluorophenylsulfonamido)-3-methyl-N-(prop-2-ynyl)butanamide for 6a–c, or CuSO₄, sodium ascorbate, 3-ethynylaniline, *t*-BuOH/EtOH/H₂O for 4; (v) toluene, 120 °C, 3 d.

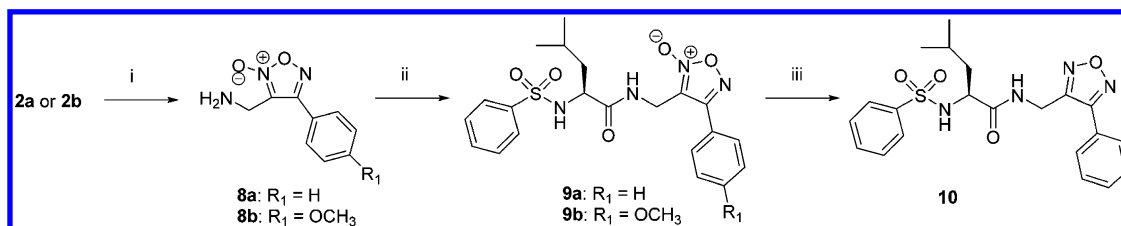
neuroprotective effects of NO, support the development of NO mimetics for the treatment of neurodegeneration and AD.^{28,34} While physiological concentrations of NO are essential for neuronal function, high concentrations of NO may lead to cell death. Therefore, an ideal neuroprotective and procognitive NO mimetic would possess the ability to produce a lower flux of NO over a sustained period of time. In this context, a furoxan with attenuated reactivity, as a thiol-dependent, nonspontaneous NO donor, is of interest (Scheme 1). To date, limited attempts have been made to modulate furoxan reactivity, and no reports have appeared on therapeutic applications in the CNS.

In this paper, the design, synthesis, and evaluation of peptidomimetic furoxans as attenuated NO-mimetic neuroprotective agents was explored for the first time. Neuroprotection was indeed observed for furoxans, whereas an analogous thiophilic furazan analogue that cannot release NO was neurotoxic. Upon coinubation of one furoxan with a sGC inhibitor, 1H-[1,2,4]oxadiazolo[4,3-*a*]quinoxalin-1-one (ODQ), the neuroprotective activity was abolished, implicating activation of the NO/sGC cascade as a key mechanistic pathway. Study of cysteine-mediated bioactivation of furoxans further supported a NO-mediated mechanism, as cysteine consumption did not correlate with NO₂⁻ production. One neuroprotective NO-donating furoxan restored normal LTP in hippocampal slices treated with oligomeric Aβ, replicating previous data on restoration of synaptic plasticity and reversal of cognitive deficits caused by oligomeric Aβ through a NO/sGC/CREB pathway.^{28,37}

RESULTS AND DISCUSSION

Design and Synthesis. The initial synthetic strategy, to produce a variety of furoxans using divergent synthesis, started from the aryl furoxan alcohols (1a–c) (Scheme 2). Furoxans incorporating classical electron donating (*p*-OCH₃, 1b) and electron withdrawing (*p*-NO₂, 1c) groups were designed to examine the effect of modifying furoxan ring reactivity via manipulations of electronic properties of the conjugated aryl system. The 4-arylfuroxan-3-methanol compounds were prepared by cyclization of the corresponding arylcinnamyl alcohols by the action of sodium nitrite in acetic acid to yield the corresponding 4-arylfuroxan-2N-oxide alcohols. The alcohols were then activated using tosyl chloride to allow conversion to the 4-arylfuroxan-2N-oxide azides (2a–c) using NaN₃ in DMF at 60 °C.

Furoxan reactivity is presumed to be most sensitive to changes in direct substitution of the furoxan ring and its conjugated systems. Contrary to modifications made in substitution of the conjugated aryl system, a methylene linker was maintained opposite to the aryl system in order to minimize potential effects on reactivity by derivatization at this end of the molecule. Recent evidence has shown the utility of nonselective cysteine protease inhibitors for neurodegenerative diseases,^{38,39} and it was speculated that a peptidomimetic thiophilic furoxan may hold the potential to inhibit cysteine proteases by direct reaction with active site cysteines. This would allow inhibition of cysteine proteases associated with neurodegeneration, concomitant with NO release. However, before study of such a hypothesis, it was necessary to

Scheme 3^a

^aReagents and conditions: (i) PPh₃, 35% NH₄OH, DMF, rt; (ii) EDCl, DMAP, (S)-4-methyl-2-(phenylsulfonamido)pentanoic acid, CH₂Cl₂, 0 °C; (iii) 9a, Zn, ammonium formate, MeOH, 60 °C.

investigate the effects of attenuated furoxans on neurons and synapses, which is the focus of the current work.

Peptidomimetic scaffolds were designed incorporating a putative recognition motif, while having negligible impact on the reactivity of the furoxan ring itself and allowing a divergent synthetic approach. Terminal alkynes were synthesized using standard peptide coupling procedures (see Supporting Information for full experimental details) and then reacted with 2a–c through a 2,3-dipolar cycloaddition to yield the corresponding furoxan-triazole containing derivatives 3–5, as well as a subset of analogues containing *p*-substituted arenes (6a–c). The peptidomimetic oxadiazole-2*N*-oxides (6a–c) were then tautomerized in boiling toluene to afford 7a–c. Additionally, 2a and 2b were converted to their corresponding amines (8a–8b) via a Staudinger reduction followed by DMAP catalyzed coupling to a peptidomimetic synthon to give 9a–9b (Scheme 3). The furazan analogue 10 was produced by treatment of 9a with a combination of activated zinc and ammonium formate at reflux.⁴⁰

Crystallography. Although the oxadiazole-*N*-oxide ring configuration can typically be assigned by comparing shifts of C₃ and C₄ of the furoxan ring by ¹³C NMR, further analysis is useful to confirm the position of the *N*-oxide moiety. Crystallographic examination of 6c revealed two independent molecules in the asymmetric unit (Figure 1), confirming the presence of the oxadiazole-2*N*-oxide structure as well as the stereochemistry of the L-valine residue incorporated into the molecule (see Supporting Information for full crystallographic details).

Reactivity. Attenuating the reactivity of the furoxan ring through structural modification is of paramount importance in NO-mimetic design. The majority of benzofuroxans are not expected to release NO on the basis of a study by Medana and co-workers separately measuring NO₂⁻, N₂O, and NO.⁴¹ In contrast, the formation of both NO and nitrosothiols from furoxans has been postulated from attack of thiolate anion; the furoxan impramidil was reported to yield nitrite, nitrate, and a bis-oxime containing product.^{4,42,43} The exact mechanism of furoxan degradation leading to NO bioactivity has not been defined and is beyond the scope of the present work. A putative mechanism is shown in Figure 2 for reaction of the furoxan 9a with cysteine. In this mechanism: (1) formation of a keto-oxime E necessarily requires loss of a nitrogen oxide (NO_x), (2) thiol may be regenerated after initial ring-opening, resulting in C, and (3) initial ring-opening may result in thiol oxidation to form a disulfide, producing B. Therefore, in the reaction of furoxan with thiol, the consumption of thiol is not intrinsically correlated with release of NO_x.

Support for the mechanism shown in Figure 2 was gained from study of the reaction of the furoxan 9a at physiological pH

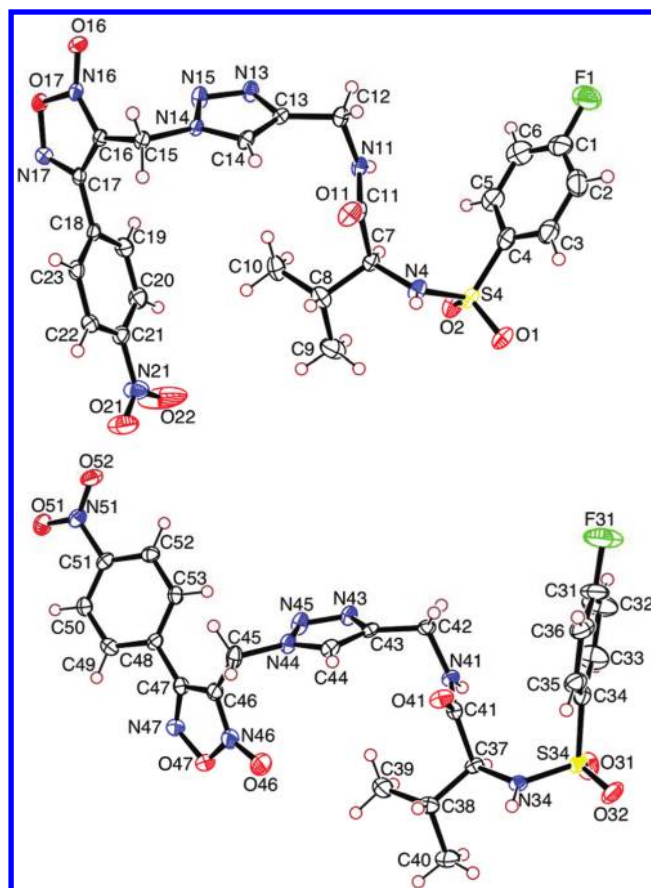


Figure 1. Crystal structure of 6c confirming the oxadiazoles-2*N*-oxide ring configuration.

and temperature in the presence of excess cysteine. After 2 h reaction, products were identified by HPLC-MS/MS (Figure 2); the parent and daughter ions of the major product were compatible with the bis-oxime hydrate D. The product corresponding to the keto-oxime, E (or its enol tautomer), and loss of NO_x constituted 11% of the reaction mixture. A compound corresponding to a cysteine-containing product (A) was observed but constituted <1% of products from integration of the UV absorbance chromatogram.

The comparable reaction of cysteine (2.5 mM) at pH 7.4 (PBS, 50 mM) and 37 °C was studied with 6a–c. After LC-MS/MS identification of products, integration of the UV absorbance chromatogram was used to quantify unreacted furoxan starting material. The rate of reaction with cysteine was observed to be lower for 6a–c than that of 9a based upon the % of starting material remaining: 9a, 11%; 6a, 68%; 6b, 75%; 6c, 14% (see Supporting Information for additional chromato-

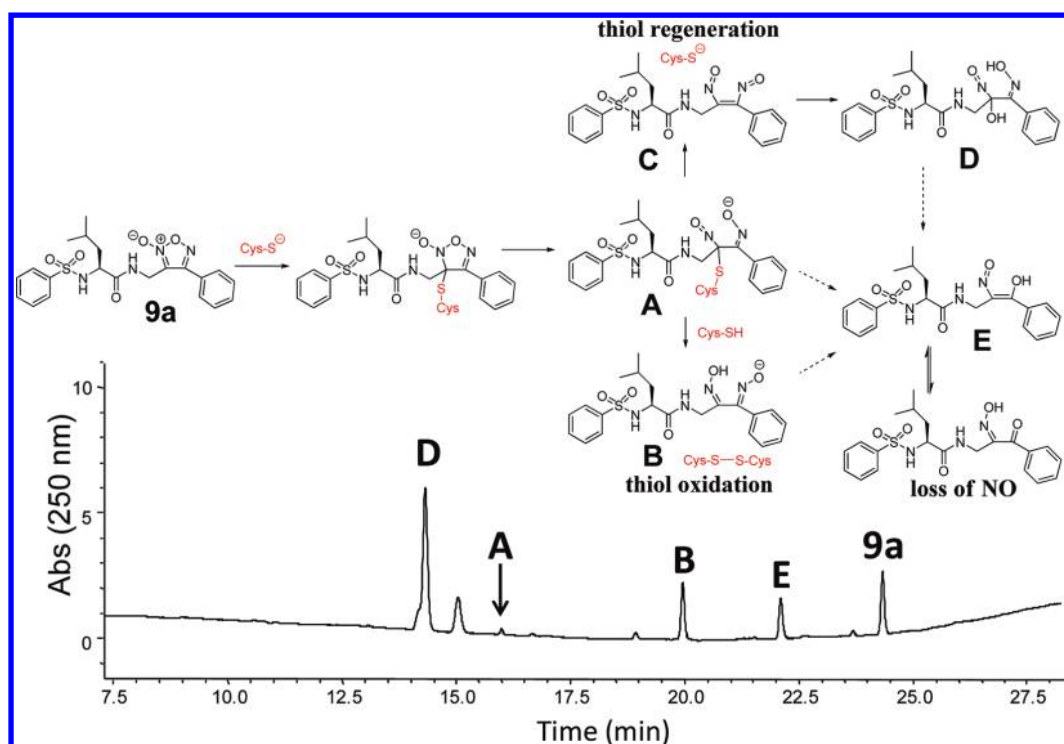
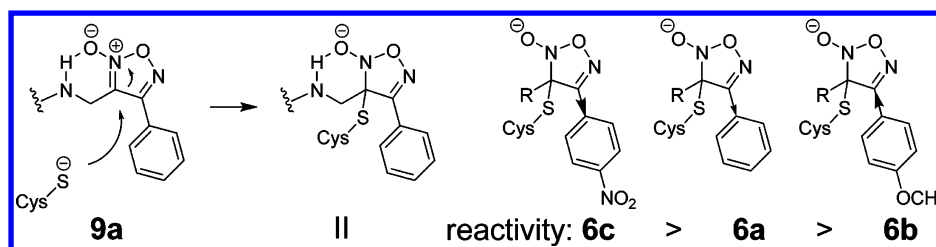


Figure 2. Putative mechanism describing reaction products observed using UV absorbance chromatogram at 250 nm for **9a** (75 μ M) in the presence of excess cysteine (5 mM) in PBS (50 mM, pH 7.4) at 37 $^{\circ}$ C for 2 h. Approximate % of products determined by integration of UV absorbance peaks. Structures proposed based on LC-MS/MS analysis of parent and daughter ions.

Scheme 4^a



^aTrend in reactivity based on % remaining parent furoxan (75 μ M) after 2 h incubation with excess cysteine (2.5 mM) in PBS (50 mM, pH 7.4) at 37 $^{\circ}$ C. Analyzed by HPLC-UV ($\lambda=250$ nm).

grams and analysis). The higher reactivity of **9a** is compatible with intramolecular stabilization of the developing negative charge in intermediate **II**, which has previously been reported to accelerate furoxan breakdown (Scheme 4).^{44,45} More importantly, the predicted modulation of reactivity by substitution of the phenyl ring, with electron-donating (**6b**) or electron-withdrawing (**6c**) substituents, was validated by the data. Thus, analysis of the reaction products from **6a–c** demonstrated that structural modification modulates overall furoxan reactivity.

NO₂⁻ Production and Cysteine Depletion. The analysis of the reaction of **9a** with cysteine identified reaction products expected for thiol regeneration, thiol oxidation, and loss of NO_x. It has been reported previously that formation of inorganic nitrite, as a measure of NO_x release, in the presence of excess cysteine (5 mM), showed reasonable correlation with vascular tissue relaxation for a series of furoxans.⁴⁶ In a similar fashion, the Griess assay for NO₂⁻ was used to analyze reactions of furoxans (250 μ M) with cysteine (2.5 mM) in a 1:1 solution of CH₃CN:PBS (50 mM, pH 7.4) at 37 $^{\circ}$ C after 24 h. Additional kinetic examination of NO₂⁻ production was carried

out (see Supporting Information), and the rate of NO₂⁻ production corresponds with quantitative NO₂⁻ production, which plateaus after 24 h. In agreement with the reported stability of furoxans in aqueous media, control incubations performed under identical conditions in the absence of cysteine gave no measurable NO_x production (data not shown).

The furoxans studied yielded between 2 and 80% mol equivalent of NO₂⁻ over the reaction time studied (Table 1). The oxadiazole-2*N*-oxides **6a–c** yielded considerably more NO₂⁻ than the tautomeric **7a–c**. The *p*-OCH₃ substituted furoxans (**4**, **5**, and **6b**) also gave much larger amounts of NO₂⁻ compared to both the tautomeric, **7a–c**, and the methylenamine-containing **9a–b**. For comparison, the bioactivation of a well studied α -cyano-furoxan, 3-cyano-4-phenyl-1,2,5-oxadiazole 2-oxide (**11**), was analyzed under similar conditions. A recent extensive study of furoxans as antiparasitic agents, converged on **11** and other α -cyano-furoxans as drug candidates.⁴⁷ Previous studies of α -cyano-furoxans as anticancer agents also included observations of cytotoxicity.⁴⁸ As might be expected if higher concentrations of NO_x lead to toxicity, **11** generated large amounts of NO₂⁻ on reaction with cysteine.

Table 1. NO_2^- Production from Furoxans after 24 h with Excess Cysteine

compd	NO_2^- production (μM) ^a	NO_2^- production as % (mol/mol) ^b
2a	9.2 (± 0.1)	18.4
2b	5.1 (± 0.1)	10.4
2c	14.8 (± 0.8)	29.6
3	40.1 (± 0.8)	80.2
4	6.3 (± 0.1)	12.6
5	9.7 (± 0.1)	19.4
6a	6.8 (± 0.1)	13.6
6b	3.9 (± 0.7)	7.8
6c	21.8 (± 0.5)	43.6
7a	1.0 (± 0.4)	2.0
7b	1.8 (± 0.1)	3.5
7c	1.3 (± 0.1)	2.5
9a	1.2 (± 0.2)	2.4
9b	0.5 (± 0.1)	1.0
10	0.0 (± 0.1)	0
11	29.1 (± 0.3)	58.2

^aQuantitative amount of NO_2^- produced from 250 μM of compound after 24 h in the presence of excess cysteine (2.5 mM) in PBS (50 mM, pH 7.4) at 37 °C; quantified using calibration curve generated with NaNO_2^- using the Griess assay. ^b NO_2^- production represented as % mol/mol.

Again as anticipated, the furazan **10** provided a negative control for NO_2^- release.

NO-mediated S-nitrosation of active site cysteines is an important step in the regulation of several proteins involved in cytoskeletal remodeling and cellular apoptosis.^{49–51} Moreover, S-nitrosation may potentially result in NO facilitated cysteine oxidation, leading to mixed disulfide formation. As discussed earlier, thiol-induced breakdown of furoxans may lead to thiol oxidation, thiol regeneration, or thiol alkylation. DTNB (5,5'-dithiobis-2-nitrobenzoic acid or Ellmans Reagent) was used to quantify free, reduced cysteine after incubation of selected furoxans (250 μM) with cysteine (2.5 mM). In normoxic solution, air oxidation of cysteine in the absence of furoxan leads to complete loss of reduced thiol within 12 h, and a high degree of background cysteine oxidation was observed upon incubation of cysteine with selected furoxans over 4 h (see Supporting Information).

To obtain a more quantitative measure of furoxan-mediated cysteine consumption, oxygen was depleted by bubbling with O_2 -free N_2 in sealed reaction vials, followed by assay of free cysteine after reaction for 2 h (Table 2). A plot of cysteine consumption versus NO_2^- production did not show a correlation (Figure 3). For example, of the substituted-phenyl furoxans, **6c** gave the highest amounts of NO_x release but the lowest cysteine consumption, confirming the disconnection between thiol consumption and NO_x release, which is predicted by the mechanism shown in Figure 2.

Neuroprotection. Neuroprotection was evaluated by 3-(4,5-dimethylthiazol-2-yl)2,5-diphenyl-tetrazolium bromide (MTT) assay of cell viability in primary rat neuronal cell cultures subjected to oxygen glucose deprivation (OGD).⁵² OGD provides a cellular model of ischemia and reperfusion injury leading to apoptotic cell death, providing a model for excitotoxic loss of neurons in neurodegenerative diseases such as ischemic stroke and AD.⁵³ Neurons were subjected to OGD for 2 h, followed by reoxygenation and replacement with nutrient rich media containing furoxans (50 μM) or vehicle

Table 2. Cysteine Remaining after 2 h Incubation with Furoxans under Hypoxic Conditions

compd	Cys as free thiol (mM) ^a	Cys depletion as % (mol/mol) ^b
–	2267.2 (± 153.7)	
4	1788.8 (± 18.7)	21.1
5	1410.1 (± 23.8)	37.8
6a	1790.8 (± 38.6)	21.0
6b	1830.4 (± 16.6)	19.2
6c	1995.2 (± 26.1)	12.0
7a	1724.4 (± 26.1)	23.9
7b	1507.2 (± 29.5)	33.5
7c	1620.4 (± 26.6)	28.5
9a	1812.1 (± 33.4)	20.1
9b	1724.4 (± 59.0)	23.9
10	1742.8 (± 23.3)	23.1

^aFree cysteine remaining in incubations containing furoxans (250 μM) and cysteine (2.5 mM) after 2 h under hypoxic conditions at 37 °C in PBS (50 mM, pH 7.4)/ CH_3CN (1:1), with 1 mM EDTA. ^bCysteine depletion relative to the control, represented as percent cysteine depletion mol/mol.

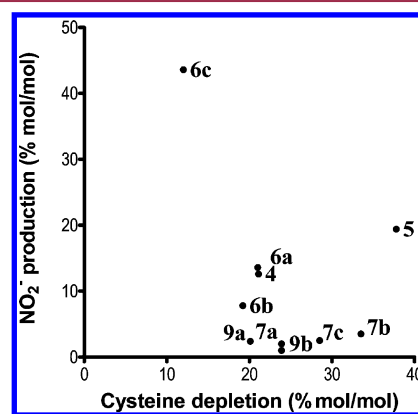


Figure 3. Correlation between NO_2^- production (% mol/mol) and cysteine depletion under hypoxic conditions (% mol/mol). NO_2^- measured using Griess assay and cysteine depletion determined using DTNB.

control. After 24 h incubation, considerable neuroprotective activity was seen for several compounds (Figure 4A), including the **6a–c** and **7a–c** subsets, which demonstrated relative neuroprotection in a manner that reflected the relative reactivity of these analogues described in Scheme 4. **E-64**, a well characterized neuroprotective cysteine protease inhibitor,^{54–56} was used as a positive control and gave significant neuroprotection. The methylenamine containing **9a** and **9b** were also shown to increase neuronal survival by 32% and 22%, respectively. The neuroprotection elicited by **9a** and **9b** suggests that even low amounts of NO_x generation are capable of eliciting a biological response. Compound **3** was not tested for neuroprotection due to limitations in aqueous solubility. Interestingly, while the majority of compounds showed significant neuroprotective activity, a few furoxans showed toxicity, including the azide family (**2a–c**) that elicited a ~50–75% loss of viability compared to the DMSO vehicle control, and the carbazole derivative, **5**, which resulted in total cell death and reduced the MTT response to baseline levels (data not shown). Furthermore, the furazan analogue, **10**, was also observed to be toxic. Because furazans are thiophilic but cannot release NO_x , this would again support a mechanism of

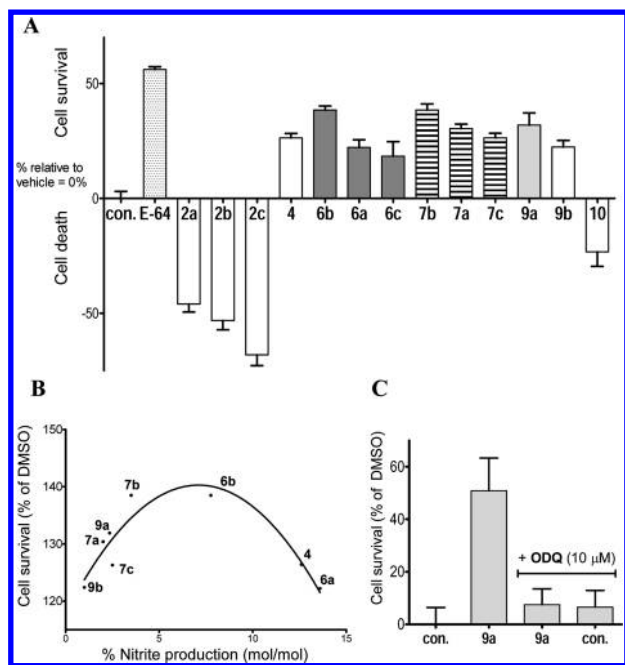


Figure 4. (A) Effect of selected furoxans on cell survival in primary rat cortical neurons. Cells treated with compound (50 μM) for 24 h following 2 h of OGD. Values represent survival as % of DMSO treated control from MTT assay. (B) Tentative correlation between NO_2^- production (% mol/mol) and cell survival (% of control). (C) Effect on cell survival in primary rat cortical neurons by DMSO treated control, the furoxan **9a** (50 μM), **9a** (50 μM) + ODQ (10 μM), and ODQ (10 μM) treated control. Values represent survival as % of DMSO treated control from MTT assay.

neuroprotection via NO_x production, rather than other mechanisms dependent on oxidation or alkylation of active site protein thiols, such as those of cysteine proteases (i.e., calpain, cathepsin B, or apoptotic caspases). A trend between NO_2^- release and neuroprotection was tentatively identified (Figure 4B). This correlation is in agreement with the concept that low levels of NO are essential for normal neuronal physiological activity, whereas high concentrations of NO can lead to cellular apoptosis and cell death. Notable outliers from this tentative correlation (5, 6c) require special considerations: (1) compounds may possess cytotoxic or neuroprotective activity through pathways other than NO signaling, and this seems to be the case for the highly toxic furoxan 5, (2) although NO_2^- production by furoxans has been reported to correlate with NO-derived bioactivity, the formation of NO_2^- is possible via routes that do not involve NO itself as an intermediate. Furoxan 6c would be predicted to be toxic based upon high levels of NO_2^- formation, however, the product profile from reaction with cysteine is very different from other furoxans studied, including unique N,O-containing intermediates that may be responsible for the copious NO_2^- production observed (see Supporting Information for detailed discussion).

Further support for the involvement of the NO/sGC pathway was obtained using ODQ, a potent and selective sGC inhibitor: after OGD, primary neurons were incubated with **9a** (50 μM) with or without ODQ (10 μM). Blockade of cGMP formation by ODQ completely abolished the neuroprotective activity observed for **9a** alone (Figure 4C), while treatment with ODQ in control groups showed no significant impact on cell survival or toxicity. These findings strongly support the involvement of a cGMP-dependent neuro-

protective mechanism driven by NO_x production from an attenuated furoxan core and are consistent with data presented below from ex vivo LTP experiments.

LTP Restoration. LTP in the Schaffer collateral pathway of the hippocampus is a cellular model of learning and memory (for review see ref 57), which is significantly impaired after perfusion with oligomers of $A\beta$.⁵⁸ $A\beta$ induced inhibition of LTP is reversed by diazeniumdiolate NO-donors via a mechanism shown to be mediated by the NO/sGC signaling pathway.²⁸ CREB is essential for memory consolidation and NO has been shown to activate CREB and to induce phosphorylation by cGMP-dependent kinase activation.⁵⁹ The peptidomimetic furoxan **9a** was selected for study of LTP restoration in hippocampal slices on the basis of: (1) an excellent neuroprotection profile (Figure 4A) (2) the confirmed involvement of the NO/sGC pathway in the mechanism of **9a** (Figure 4C), and (3) desirable physicochemical properties for CNS bioavailability compared to the other furoxan analogues studied (MW < 450, clogP = 2.9). It was hypothesized that **9a** should possess the ability to restore synaptic function in hippocampal slices copperfused with oligomeric $A\beta$. In accordance with previous data and the hypothesis that NO_x release from furoxans is able to restore brain function, **9a** (1 μM) was found to completely abrogate $A\beta$ induced synaptic deficits in LTP; synaptic response to LTP induction was restored to levels matching those of untreated wild-type controls (Figure 5). This novel bioactivity of furoxans implicates the NO/sGC/CREB pathway as being activated in hippocampal slices, in simile with

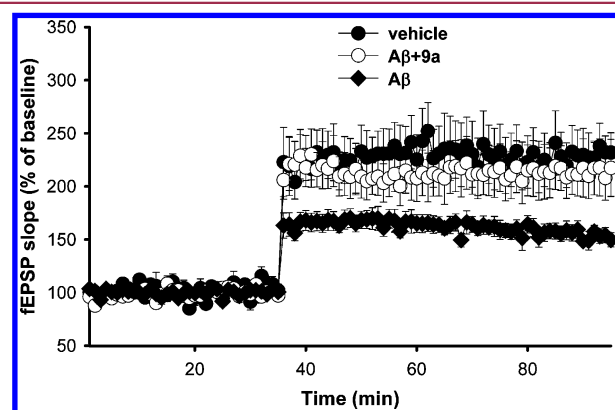


Figure 5. Restoration of long-term potentiation by **9a** (1 μM) in hippocampal slices perfused with oligomeric $A\beta$ (200 nM) (for each experiment $n = 7$).

other NO-donors and further supports development of furoxans as therapeutics in dementia and neurodegeneration.

CONCLUSION

The NO-mimetic furoxan ring was incorporated into a series of peptidomimetic scaffolds; one novel approach used click chemistry to demonstrate the potential for synthetic elaboration of this novel peptidomimetic drug class. It was postulated that substitution of the furoxan ring would lead to modulation of reactivity toward thiol-mediated bioactivation, and further, that attenuation of reactivity would unmask the cytoprotective properties of NO. This was deemed important because cytotoxicity has been associated with the higher fluxes of NO deriving from known furoxan anti-infective agents. Attenuation of reactivity and propensity for NO release was accomplished by appropriate substitution of the furoxan ring. Neuro-

protection by furoxans in primary rat neurons subjected to ischemia-reperfusion injury correlated with NO_2^- production but did not correlate with loss of free thiol. Neuroprotection was abolished by coincubation with the sGC inhibitor, ODQ, implicating the involvement of the NO/sGC cascade. One furoxan, **9a**, was observed to restore LTP following an $\text{A}\beta$ -induced synaptic deficit in mouse hippocampal slices, compatible with the known capacity of NO/sGC/CREB activation to restore LTP. As a whole, these findings strongly suggest activation of the NO/sGC/CREB cascade as the primary mechanism of furoxan elicited neuroprotection and synaptic function restoration. Future efforts to develop attenuated furoxans for the CNS should focus on developing substitution patterns that decrease the reactivity of the furoxan ring itself. The work represents the first description of furoxans as neuroprotective and procognitive agents with potential application in stroke and AD.

EXPERIMENTAL SECTION

All chemicals and reagents were purchased from Sigma-Aldrich (St. Louis, MO), or Fisher Scientific unless stated otherwise.

Crystallography. The furoxan (**6c**) was chosen for crystallographic examination. Molecular formula, $\text{C}_{23}\text{H}_{23}\text{FN}_8\text{O}_7\text{S}$; formula weight, 574.1418; crystal system, orthorhombic, $P2_12_12_1$ (#19) with unit cell dimensions $a = 11.334$ (1) Å, $b = 21.427$ (2) Å, $c = 21.643$ (1) Å; volume = 5256.1 (6) Å³; Z , calculated density = 8, 1.452 mg/m³; absorption coefficient = 0.190 mm⁻¹. A colorless needle, with dimensions $2 \times 2 \times 40$ μm³, was selected for data collection. The crystal was cooled to 100 K and aligned in the X-ray beam at sector 22 (SER-CAT) on the ID beamline at the Advanced Photon Source at Argonne National Lab. Data collection was carried out at a wavelength of 0.80 Å using 5° rotations and exposure time of 1 s and collected with a MAR 300 mm CCD detector. Then 72 images were indexed and integrated using XDS and averaged over mmm symmetry. The structure was solved using SHELX-97 and refined using WinGX and SHELXL; ORTEP was used to generate the molecular figures. Hydrogen atoms were added to the model in idealized positions. The final model gave agreement factors (R indices) of $R1 = 0.0407$, $wR2 = 0.1030$. We observed two independent molecules in the asymmetric unit, confirming the presence of the oxadiazole-2*N*-oxide structure within the structures.

Reactivity Analysis. The appropriate furoxan (75 μM) was incubated with L-cysteine (2.5 mM) in PBS (50 mM, pH 7.4) at 37 °C for 2 h. The products were then separated and analyzed by HPLC-MS/MS. Peak integration from UV absorbance spectra gives the estimated relative abundance of each reaction product and is correlated with the TIC chromatogram to identify peaks by MS/MS analysis.

Griess Assay. The parent furoxan (250 μM) was dissolved in PBS (50 mM, pH 7.4)/CH₃CN (1:1); L-cysteine (2.5 mM) was added and the mixture incubated at 37 °C for 24 h. Aliquots (taken at 1, 2, 4, 8, 12, 18, and 24 h) were incubated for 10 min with Griess reagent A (1.0% sulfanilamide, 5.0% H₃PO₄ in dH₂O)/griess reagent B (0.1% (*N*-1-naphthyl)ethylenediamine dihydrochloride in dH₂O). UV absorbance at 530 nm was measured using a Dynex MRX II microplate spectrophotometer and calibrated using a standard curve constructed with NaNO₂ to yield nitrite concentration.

Cysteine Reactivity. The parent furoxan (250 μM) was dissolved in a solution of PBS (50 mM, pH 7.4, over Chelex 100)/CH₃CN (1:1) containing EDTA (1%) and the mixture purged with N₂ for 10 min; L-cysteine (2.5 mM) was added and the mixture purged with N₂ for an additional 5 min followed by incubation at 37 °C for 2 h. Aliquots were mixed with DTNB (750 μM, in PBS 50 mM, pH 7.0) for 5 min. UV absorbance of DTNB mixture was measured at 412 nm using a Dynex MRX II microplate spectrophotometer and calibrated using a standard curve constructed using L-cysteine in the presence of DTNB to yield total reduced cysteine concentration.

Neuroprotection Assay. Use of animals was approved by the Institutional Animal Care and Use Committee at the University of Illinois at Chicago. Cell cultures were prepared from the cortex and hippocampus of rat embryos at 16–18 d of gestation and grown in neurobasal media supplemented with B27 and glutamine, a technique shown to result in a population of greater than 99% pure neurons.⁵⁹ After 9–11 DIV, cultures were transferred to hypoxic chamber (Coy Lab, Grass Lake, MI; dimensions 41" L × 23" D × 23" H) with an atmosphere of 5% CO₂/95% N₂; oxygen tension being monitored by electrode and kept to less than 1%. Culture media was replaced with a salt-balanced solution containing the following (in mM): NaCl 116, CaCl₂ 1.8, MgSO₄ 0.8, KCl 5.4, NaH₂PO₄ 1, NaHCO₃ 14.7, HEPES 10. After 2 h, cells were removed from hypoxic chamber and resupplied with neurobasal media and compounds at 50 μM or vehicle control with or without ODQ (10 μM). After 24 h of incubation, cell survival assay was performed by addition of MTT at 250 ng/mL, followed by a 3 h incubation, followed by media aspiration and dissolution of insoluble dye crystals in acidified organic propanol, with final reading of absorbance performed on an ELISA plate reader at 590 nm.

LTP Assay. Mice were decapitated and their hippocampi were rapidly dissected out. then 400 μm slices were cut with a tissue chopper and maintained in an interface chamber at 29 °C for 90 min prior to recording. Slices were perfused with artificial CSF (in mM): NaCl 124, KCl 4.4, Na₂HPO₄ 1.0, NaHCO₃ 25, CaCl₂ 2.0, MgSO₄ 2.0, and glucose 10, which was continuously bubbled with 95% O₂ and 5% CO₂. Slices were permitted to recover from cutting for at least 90 min before recordings. The fEPSPs were recorded from the CA1 region of the hippocampus by placement of both the stimulating and the recording electrodes in the CA1 stratum radiatum. Following recording of a 15 min baseline in which individual fEPSP were recorded every min at an intensity that evokes a response ~35% of the maximum evoked response, compounds and β-amyloid were perfused for 20 min prior to LTP induction. LTP was elicited through a θ-burst stimulation: 4 pulses at 100 Hz, with the bursts repeated at 5 Hz and each tetanus including 3 ten-burst trains separated by 15 s.

General Methods. Unless stated otherwise, all reactions were carried out under an atmosphere of dry argon in oven-dried glassware. Indicated reaction temperatures refer to those of the reaction bath, while room temperature (rt) is noted as 25 °C. Dichloromethane (CH₂Cl₂) was distilled over CaH₂ and THF distilled over Na(s). All other solvents were of anhydrous quality purchased from Aldrich Chemical Co. and used as received. Commercially available starting materials and reagents were purchased from Aldrich, TCI, and Fisher Scientific and were used as received unless specified otherwise. *trans*-Epoxy succinyl-L-leucyl-amido(4-guanidino) butane (**E-64**), 1*H*-[1,2,4]-oxadiazole[4,3-*a*]quinoxalin-1-one (ODQ), and 4-phenyl-3-fuxoxan-carbonitrile (**11**) were purchased from Sigma and used as received. Analytical thin layer chromatography (TLC) was performed with (5 cm × 20 cm, 60 Å, 250 μm). Visualization was accomplished using a 254 nm UV lamp. ¹H and ¹³C NMR spectra were recorded on either a Bruker Avance 400 MHz spectrometer or Bruker DPX 400 MHz spectrophotometer. Chemical shifts are reported in ppm with the solvent resonance as internal standard ([CDCl₃ 7.27 ppm, 77.23 ppm], [DMSO-*d*₆ 2.5 ppm, 39.51 ppm], and [MeOD-*d*₄ 4.78, 49.0] for ¹H, ¹³C, respectively). Data are reported as follows: chemical shift, multiplicity (s = singlet, d = doublet, dd = doublet of doublet, t = triplet, q = quartet, br = broad, m = multiplet, abq = ab quartet), number of protons, and coupling constants. Low-resolution mass spectra (LRMS) were acquired on an Agilent 6310 Ion-Trap LC/MS. High resolution mass spectral (HRMS) data was collected in-house using a Shimadzu QTOF 6500. All compounds submitted for biological testing were found to be >95% pure by analytical HPLC. Purity and/or low resolution mass spectral (ESI or APCI) analysis was measured using an Advantage ARMOR C18; 5 μM; 150 mm × 4.6 mm analytical column on either a Shimadzu UFLC (Instrument 1) or Agilent 1100 Series HPLC in tandem with an Agilent 6310 Ion Trap LC/MS (Instrument 2). HPLC method: solvents, 0.05% FA in CH₃CN (solvent A); 0.05% FA in 9:1 mixture of H₂O and MeOH (solvent B); flow rate 1.0 mL/min. Gradient: $t = 0$ min, 10% B; $t = 5$

min, 30% B; $t = 15$ min, 70% B; $t = 30$ min, 90% B; $t = 35$ min, 50% B, $t = 38$, 10% B. Stop time 45 min.

General Procedure for Arylfuroxan-3-methanol Cyclization. The appropriate cinnamyl alcohol (100 mmol) was dissolved in acetic acid (25 mL) under argon at 0 °C. NaNO_2 (300 mmol) was added portionwise over 30 min while maintaining reaction temperature <20 °C. The reaction was then allowed to warm to rt and monitored by TLC. After 4 h, the reaction was diluted with ice water and extracted with ethyl acetate (3×175 mL). The combined organic extracts were washed with brine (2×75 mL), dried over Na_2SO_4 , and concentrated to afford orange oil. The residual oil was then purified by column chromatography (hexane/ethyl acetate [10:1 \rightarrow 5:1]) to yield the desired products in each circumstance as described below.

3-(Hydroxymethyl)-4-phenyl-1,2,5-oxadiazole 2-Oxide (1a). Yellow solid (4.8 g, 24.9%). ^1H NMR (CDCl_3 , 400 MHz): δ 7.85–7.82 (m, 2H), 7.61–7.54 (m, 3H), 4.77–4.76 (d, 2H, $J = 4.89$ Hz), 2.82 (bs, 1H). ^{13}C NMR (CDCl_3 , 100 MHz): 157.05, 131.58, 130.38, 129.62, 129.36, 127.99, 126.36, 115.07, 56.93.

3-(Hydroxymethyl)-4-(4-methoxyphenyl)-1,2,5-oxadiazole 2-Oxide (1b). White solid (5.8 g, 26.1%). ^1H NMR (CDCl_3 , 400 MHz): δ 7.79–7.77 (d, 2H, $J = 9.75$ Hz), 7.08–7.02 (d, 2H, $J = 9.75$ Hz), 4.77–4.75 (d, 2H), 3.90–3.86 (s, 3H), 2.64–2.60 (t, 1H). ^{13}C NMR (CDCl_3 , 100 MHz): 161.97, 156.48, 129.28, 118.42, 114.82, 114.74, 55.45, 53.42.

3-(Hydroxymethyl)-4-(4-nitrophenyl)-1,2,5-oxadiazole 2-Oxide (1c). White solid (6.9 g, 29.1%). ^1H NMR (CDCl_3 , 400 MHz): δ 8.44–8.42 (d, 2H, $J = 8.8$ Hz), 8.13–8.10 (d, 2H, $J = 8.8$ Hz), 4.79 (s, 2H), 2.45–2.18 (bs, 1H). ^{13}C NMR (CDCl_3 , 100 MHz): 154.75, 149.15, 131.76, 128.55, 124.15, 113.21, 52.94.

General Procedure for Alcohol Activation. Triethylamine (0.62 mL, 4.43 mmol) was added to furoxan alcohol (284 mg, 1.48 mmol) in freshly distilled CH_2Cl_2 (10 mL) at 0 °C. TsCl (380 mg, 2.2 mmol) was separately dissolved in CH_2Cl_2 (5 mL) and added dropwise over 10 min. The mixture was allowed to warm to rt and stirred for 3 h. The reaction was quenched w/saturated aqueous NH_4OH (10 mL) and extracted with ethyl acetate (3×75 mL). Combined organic layers washed with brine (2×15 mL), dried over Na_2SO_4 , and concentrated to give yellow oil. Reaction products were isolated by column chromatography (hexane/ethyl acetate [8:1 \rightarrow 4:1]). Once products were confirmed by NMR, subsequent crude mixtures of the tosyl and chloro intermediates were submitted to next reaction without further purification.

General Procedure for Preparation of the Azide. NaN_3 (1.5 equiv) was added to the a mixture of the tosyl and chloro derivatives (1.0 equiv) in DMF (10 mL) and the reaction brought to 50 °C and reaction progress monitored by TLC. After completion of reaction (typically 4–12 h), the reaction was quenched with ice water (150 mL) and extracted with ethyl acetate (3×50 mL). The combined organic extracts were washed with brine (2×50 mL), water (3×250 mL), dried over Na_2SO_4 , and concentrated to give orange oil. Crude oil was purified by column chromatography (hexane/ethyl acetate [5:1]) to give a mixture of the desired azides described below.

3-(Azidomethyl)-4-phenyl-1,2,5-oxadiazole 2-Oxide (2a). Synthesized using the general procedure with the following values. Crude mixture of tosylated and chlorinated 1a (366 mg, 1.06 mmol) and NaN_3 (100 mg, 1.6 mmol) afforded 2a as a white solid (175 mg, 76.3%). ^1H NMR (CDCl_3 , 400 MHz): δ 7.76–7.74 (d, 2H), 7.63–7.56 (m, 3H), 4.48 (s, 2H). ^{13}C NMR (CDCl_3 , 100 MHz): 156.51, 131.54, 129.51, 127.67, 125.80, 111.75, 42.83. Analytical HPLC (instrument 1): purity = 97.9%, $t_R = 22.8$ min.

3-(Azidomethyl)-4-(4-methoxyphenyl)-1,2,5-oxadiazole 2-Oxide (2b). Synthesized using general the procedure with the following values. Crude mixture of tosylated and chlorinated 1b (560 mg, 1.5 mmol) and NaN_3 (150 mg, 2.2 mmol) afforded 2b as a white solid (310 mg, 84.3%). ^1H NMR (CDCl_3 , 400 MHz): δ 7.70–7.67 (d, 2H), 7.09–7.05 (d, 2H), 4.47 (s, 2H), 3.90 (s, 3H). ^{13}C NMR (CDCl_3 , 100 MHz): 162.10, 156.20, 129.15, 118.01, 114.94, 111.71, 55.47, 42.91. Analytical HPLC (instrument 1): purity = 99.2%, $t_R = 23.5$ min.

3-(Azidomethyl)-4-(4-nitrophenyl)-1,2,5-oxadiazole 2-oxide (2c). Synthesized using the general procedure with the following values.

Crude mixture of tosylated and chlorinated 1c (612 mg, 1.63 mmol) and NaN_3 (160 mg, 2.4 mmol) afforded 2c as a white solid (345 mg, 85.8%). ^1H NMR (CDCl_3 , 400 MHz): δ 8.45–8.42 (d, 2H), 8.01–7.99 (d, 2H), 4.52 (s, 2H). ^{13}C NMR (CDCl_3 , 100 MHz): 154.68, 149.55, 131.71, 128.81, 124.65, 111.22, 42.85. Analytical HPLC (instrument 1): purity = 97.4%, $t_R = 23.4$ min.

General Procedure for Click Reaction A. The azide (25 mg, 0.12 mmol) was dissolved in toluene (5 mL) followed by under argon, by the addition of phenylacetylene (15 mg, 0.15 mmol) and copper(I) iodide (10 mg, 0.032 mmol). N,N -Diisopropylethylamine (0.02 mL, 0.115 mmol) was then added to the solution. The reaction was allowed to stir at room temperature until TLC analysis (hexane/ethyl acetate [1:1]) indicated completion. The solution was filtered through Celite and concentrated to give a crude brown solid, which was purified by column chromatography to give the title compound.

General Procedure for Click Reaction B. The furoxan azide (1.0 equiv), 3-ethynylaniline (1.0 equiv), sodium ascorbate (0.4 equiv), and CuSO_4 (0.2 equiv) were stirred in $t\text{-BuOH}/\text{EtOH}/\text{H}_2\text{O}$ (3:1:1) for 12 h. Reaction was filtered through Celite and concentrated. Residual oil was purified by column chromatography to give the title compound.

4-Phenyl-3-((4-phenyl-1H-1,2,3-triazol-1-yl)methyl)-1,2,5-oxadiazole 2-Oxide (3). Synthesized using the general click procedure with the following values. Click reaction A: furoxan-azide (25 mg, 0.12 mmol), phenylacetylene (15 mg, 0.15 mmol), copper(I) iodide (10 mg, 0.032 mmol) and N,N -diisopropylethylamine (0.02 mL, 0.115 mmol) afforded 3 as a white solid (30 mg, 81.6%). ^1H NMR ($\text{DMSO}-d_6$, 400 MHz): δ 8.69 (s, 1H), 7.83–7.81 (t, 4H), 7.61–7.59 (m, 3H), 7.44–7.31 (m, 3H), 5.81 (s, 2H). ^{13}C NMR ($\text{DMSO}-d_6$, 100 MHz): 157.46, 146.90, 131.94, 130.63, 129.82, 129.38, 128.56, 128.23, 125.84, 125.65, 122.93, 112.54, 42.62.

3-((4-(3-Aminophenyl)-1H-1,2,3-triazol-1-yl)methyl)-4-(4-methoxyphenyl)-1,2,5-oxadiazole 2-Oxide (4). Click reaction B: *p*-methoxyphenylfuroxan azide (65 mg, 0.26 mmol), 3-ethynylaniline (30.8 mg, 0.26 mmol), sodium ascorbate (20 mg, 0.1 mmol), and CuSO_4 (8 mg, 0.05 mmol) afforded 4 as a white solid (72 mg, 75.0%). ^1H NMR (CDCl_3 , 400 MHz): δ 8.02 (s, 1H), 7.87–7.84 (d, 2H, $J = 6.8$ Hz), 7.22–7.21 (t, 1H), 7.20–7.18 (d, 1H, $J = 7.63$ Hz), 7.17–7.15 (dt, 1H), 7.09–7.06 (d, 2H, $J = 6.8$ Hz), 6.68–6.55 (dq, 1H), 5.59 (s, 2H), 3.87 (s, 3H). ^{13}C NMR (CDCl_3 , 100 MHz): 162.23, 156.27, 148.81, 146.96, 130.71, 129.85, 129.65, 120.74, 117.41, 116.05, 115.28, 115.06, 112.18, 111.61, 55.47, 42.09. ESI-HRMS (m/z): $[\text{M} + \text{H}]^+$ calcd for $\text{C}_{18}\text{H}_{16}\text{N}_6\text{O}_3$, 365.1356; obsd, 365.1360. Analytical HPLC (instrument 1): purity = 97.3%, $t_R = 12.7$ min.

3-((4-((2,8-Dimethyl-3,4-dihydro-1H-pyrido[4,3-b]indol-5(2H)-yl)methyl)-1H-1,2,3-triazol-1-yl)methyl)-4-(4-methoxyphenyl)-1,2,5-oxadiazole 2-Oxide (5). Click reaction A: carbazole alkyne (26 mg, 0.105 mmol [see Supporting Information for preparation]), furoxan azide (34 mg, 0.143 mmol), DIPEA (0.03 mL, 0.18 mmol), and CuI (20 mg, 0.06 mmol) yielded 5 as a white solid (52 mg, 75.1%). ^1H NMR (CDCl_3 , 400 MHz): δ 7.79–7.76 (d, 2H, 8.83 Hz), 7.50 (s, 1H), 7.22–7.19 (m, 2H), 7.05–7.02 (d, 2H, $J = 8.83$ Hz), 7.01–6.99 (d, 1H, $J = 8.28$ Hz), 5.40 (s, 2H), 5.31 (s, 2H), 3.88 (s, 3H), 3.80 (s, 2H), 3.00 (s, 4H), 2.89 (s, 3H), 2.63 (s, 3H), 2.43 (s, 3H). ^{13}C NMR (CDCl_3 , 100 MHz): 161.81, 155.80, 145.21, 134.28, 131.96, 129.20, 128.57, 125.62, 122.65, 122.61, 117.30, 117.04, 114.65, 110.84, 108.31, 106.64, 55.09, 51.60, 51.00, 44.38, 41.67, 38.17, 21.69, 21.00. ESI-HRMS (m/z): $[\text{M} + \text{H}]^+$ calcd for $\text{C}_{26}\text{H}_{27}\text{N}_7\text{O}_3$, 486.2248; obsd, 486.2258. Analytical HPLC (instrument 1): purity = 99.0%, $t_R = 8.3$ min.

(R)-3-((4-((2-(4-Fluorophenylsulfonamido)-3-methylbutanamido)methyl)-1H-1,2,3-triazol-1-yl)methyl)-4-phenyl-1,2,5-oxadiazole 2-Oxide (6a). Click reaction A: peptidomimetic alkyne (140 mg, 0.44 mmol [see Supporting Information for preparation]), 2a (100 mg, 0.40 mmol), DIPEA (0.07 mL, 0.44 mmol), and CuI (10 mg, 0.04 mmol) yielded 6a ($R_f = 0.37$, hexane/ethyl acetate [1:2]) as a white solid (174 mg, 76.8%). ^1H NMR ($\text{DMSO}-d_6$, 400 MHz): δ 8.80–8.60 (t, 1H), 7.94 (s, 1H), 7.89–7.81 (bs, 1H), 7.89–7.76 (m, 4H), 7.65–7.58 (m, 3H), 7.34–7.29 (t, 2H), 5.72 (s, 2H), 4.19–3.93 (abq, 2H), 3.44 (bs, 1H), 1.78–1.76 (q, 1H), 0.77–0.70 (dd, 6H). ^{13}C NMR ($\text{DMSO}-d_6$, 100 MHz): 170.27,

157.41, 145.02, 131.97, 130.54, 129.95, 129.86, 128.20, 125.84, 124.34, 116.27, 116.05, 112.64, 62.25, 42.18, 34.21, 31.12, 19.36, 18.78. ESI-HRMS (m/z): $[M + H]^+$ calcd for $C_{23}H_{24}FN_7O_5S$, 530.1567; obsd, 530.1636; $[M - H]^+$ calcd for $C_{23}H_{24}FN_7O_5S$, 528.1519; obsd, 528.1541. Analytical HPLC (instrument 1): purity = 97.1%, t_R = 24.4 min.

(*R*)-3-((4-((2-(4-Fluorophenylsulfonamido)-3-methylbutanamido)methyl)-1*H*-1,2,3-triazol-1-yl)methyl)-4-(4-methoxyphenyl)-1,2,5-oxadiazole 2-Oxide (**6b**). Click reaction A: peptidomimetic alkyne (140 mg, 0.44 mmol), **2b** (100 mg, 0.40 mmol), DIPEA (0.07 mL, 0.44 mmol), and CuI (10 mg, 0.04 mmol) yielded **6b** (R_f = 0.36, hexane/ethyl acetate [1:2]) as a white solid (yield = 58%). 1H NMR (CD_3CN-d_3 , 400 MHz): δ 7.85–7.82 (q, 2H), 7.79–7.77 (d, 2H, J = 8.83), 7.69 (s, 1H), 7.24–7.20 (t, 2H), 7.15–7.13 (d, 2H, J = 8.78), 6.91 (bs, 1H), 5.93–5.91 (d, 1H, J = 8.80), 5.57 (s, 2H), 4.24–4.07 (qd, 2H), 3.89 (s, 3H), 3.55–3.47 (t, 1H), 1.95–1.78 (m, 1H), 0.82–0.79 (q, 6H). ^{13}C NMR (CD_3CN-d_3 , 100 MHz): 170.29, 163.11, 162.08, 157.02, 145.07, 137.88, 130.05, 129.95, 129.78, 124.26, 117.97, 116.27, 116.05, 115.33, 112.53, 62.26, 55.92, 49.03, 42.24, 34.23, 31.11, 19.34, 18.77. ESI-HRMS (m/z): $[M + H]^+$ calcd for $C_{24}H_{26}FN_7O_6S$, 560.1673; obsd, 560.1739; $[M - H]^+$ calcd for $C_{24}H_{26}FN_7O_6S$, 558.1625; obsd, 558.1649. Analytical HPLC (instrument 1): purity = 98.5%, t_R = 24.9 min.

(*R*)-3-((4-((2-(4-Fluorophenylsulfonamido)-3-methylbutanamido)methyl)-1*H*-1,2,3-triazol-1-yl)methyl)-4-(4-nitrophenyl)-1,2,5-oxadiazole 2-Oxide (**6c**). **2c** (200 mg, 1 mmol) dissolved in toluene (5 mL) was added the terminal alkyne (340 mg, 1.1 mmol) in 4 mL of toluene/methanol (3:1) at room temperature. To this suspension, CuI (30 mg, 0.1 mmol) was added followed by DIPEA (0.18 mL, 1 mmol) and the reaction stirred for 8 h. The reaction was then filtered through Celite and concentrated. The corresponding oil was dissolved in CH_2Cl_2 and successively washed with 1 N HCl (2 \times 15 mL), brine (2 \times 30 mL), dried over Na_2SO_4 and concentrated to give a yellow solid. The solid was then washed with $CHCl_3$, giving the desired product as a white solid (352 mg, 63%). R_f = 0.38 (hexane/ethyl acetate [1:2]). 1H NMR (DMSO- d_6 , 400 MHz): δ 8.39–8.37 (d, 2H, J = 8.0 Hz), 8.34–8.31 (t, 1H), 8.26 (s, 1H), 8.07–8.05 (d, 2H, J = 8.0 Hz), 7.92 (s, 1H), 7.85–7.83 (d, 1H, J = 9.2 Hz), 7.31–7.26 (t, 2H), 5.78 (s, 2H), 4.08–3.89 (qd, 2H), 3.42–3.38 (t, 1H), 1.76–1.71 (m, 1H), 0.73–0.66 (dd, 6H). ^{13}C NMR (DMSO- d_6 , 100 MHz): 170.29, 156.09, 149.57, 145.04, 131.77, 130.05, 129.95, 129.91, 124.81, 124.42, 116.27, 116.24, 112.66, 62.26, 34.21, 31.09, 19.34. ESI-HRMS (m/z): $[M + H]^+$ calcd for $C_{23}H_{23}FN_8O_7S$, 575.1418; obsd, 575.1477; $[M - H]^+$ calcd for $C_{23}H_{23}FN_8O_7S$, 573.1370; obsd, 573.1384. Analytical HPLC (instrument 1): purity = 95.7%, t_R = 24.7 min.

General Procedure for the Isomerization to the Tautomeric Oxadiazole-*N*-oxides. The appropriate oxadiazole-2*N*-oxide (1 mmol) was suspended in anhydrous toluene (10 mL) and heated to 120 °C for 3 d. The reaction was allowed to cool to rt, toluene removed under vacuo, and the mixture of isomers was purified by column chromatography (hexane/ethyl acetate [2:1 \rightarrow 1:2]) to give the corresponding tautomeric furoxans.

(*R*)-4-((4-((2-(4-Fluorophenylsulfonamido)-3-methylbutanamido)methyl)-1*H*-1,2,3-triazol-1-yl)methyl)-3-phenyl-1,2,5-oxadiazole 2-Oxide (**7a**). White solid (33% conversion); R_f = 0.27 (hexane/ethyl acetate [1:2]). 1H NMR ($CDCl_3$, 400 MHz): δ 7.85–7.81 (q, 2H), 7.71 (s, 1H), 7.66–7.65 (m, 2H), 7.61–7.54 (m, 3H), 7.13–7.08 (t, 2H), 6.84 (bs, 1H), 5.80–5.72 (q, 2H), 5.60–5.58 (d, 1H, J = 8.54), 4.45–4.36 (m, 2H), 3.55–3.51 (q, 1H), 2.06–2.01 (m, 1H), 0.83–0.79 (q, 6H). ^{13}C NMR ($CDCl_3$, 100 MHz): 170.55, 151.25, 145.15, 131.20, 130.08, 129.87, 129.54, 127.69, 122.78, 121.33, 116.27, 116.05, 62.24, 45.17, 34.76, 31.33, 19.09, 17.31. ESI-HRMS (m/z): $[M + H]^+$ calcd for $C_{23}H_{24}FN_7O_5S$, 530.1567; obsd, 530.1624; $[M - H]^+$ calcd for $C_{23}H_{24}FN_7O_5S$, 528.1519; obsd, 528.1557. Analytical HPLC (instrument 2): purity = 97.0%, t_R = 23.68 min.

(*S*)-4-((4-((2-(4-Fluorophenylsulfonamido)-3-methylbutanamido)methyl)-1*H*-1,2,3-triazol-1-yl)methyl)-3-(4-methoxyphenyl)-1,2,5-oxadiazole 2-Oxide (**7b**). White solid (25% conversion); R_f = 0.26 (hexane/ethyl acetate [1:2]). 1H NMR ($CDCl_3$, 400 MHz): δ 8.14–8.12 (d, 1H), 7.84–7.81 (t, 3H), 7.69 (s,

1H), 7.63–7.61 (d, 2H), 7.52–7.48 (t, 1H), 7.12–7.04 (m, 5H), 6.82 (bs, 1H), 5.76–5.74 (q, 2H), 5.59–5.50 (m, 2H), 3.60 (s, 3H), 3.54–3.51 (m, 2H), 2.10–2.02 (m, 3H), 0.82–0.79 (q, 6H). ^{13}C NMR ($CDCl_3$, 100 MHz): 170.50, 161.57, 151.4, 145.07, 135.48, 133.57, 130.13, 130.01, 129.23, 128.47, 122.60, 116.27, 116.04, 115.06, 62.20, 55.47, 45.29, 34.73, 31.38, 29.67, 19.09, 17.27. ESI-HRMS (m/z): $[M + H]^+$ calcd for $C_{24}H_{26}FN_7O_6S$, 560.1673; obsd, 560.1723; $[M - H]^+$ calcd for $C_{24}H_{26}FN_7O_6S$, 558.1625; obsd, 558.1664. Analytical HPLC (instrument 2): purity = 95.9%, t_R = 23.9 min.

(*R*)-4-((4-((2-(4-Fluorophenylsulfonamido)-3-methylbutanamido)methyl)-1*H*-1,2,3-triazol-1-yl)methyl)-3-(4-nitrophenyl)-1,2,5-oxadiazole 2-Oxide (**7c**). White solid (52% conversion); R_f = 0.28 (hexane/ethyl acetate [1:2]). 1H NMR ($CDCl_3$, 400 MHz): δ 8.41–8.39 (d, 2H, J = 8.96), 7.96–7.94 (d, 2H, J = 8.96), 7.86–7.82 (q, 2H), 7.77 (s, 1H), 7.17–7.13 (t, 2H), 6.76 (bs, 1H), 5.84–5.76 (q, 2H), 5.41–5.39 (d, 1H, J = 8.00), 4.46–4.41 (q, 2H), 3.50–3.46 (q, 1H), 2.06–2.01 (m, 1H), 0.80–0.78 (q, 6H). ^{13}C NMR ($CDCl_3$, 100 MHz): 170.69, 150.75, 148.82, 145.70, 130.09, 130.00, 128.77, 124.54, 122.81, 116.40, 116.17, 112.81, 62.36, 60.38, 45.12, 34.90, 31.07, 19.07, 17.26, 14.17. ESI-HRMS (m/z): $[M + H]^+$ calcd for $C_{23}H_{23}FN_8O_7S$, 575.1418; obsd, 575.1456; $[M - H]^+$ calcd for $C_{23}H_{23}FN_8O_7S$, 573.1370; obsd, 573.1380. Analytical HPLC (instrument 2): purity = 95.1%, t_R = 24.2 min.

General Procedure for Staudinger Reduction, Yielding **8a and **8b**.** The appropriate azide (1 equiv) and $P(Ph)_3$ (15.8 equiv) were dissolved in DMF and stirred at rt for 1 h. Then 35% NH_4OH (4 equiv) was added dropwise and reaction continued for an additional hour. The mixture was then diluted with ice water and extracted with ethyl acetate (3 \times 100 mL). Combined organic layers were then extracted with 1 N HCl (3 \times 100 mL). Combined acidic extracts were washed with $CHCl_3$ (3 \times 75 mL), brought to pH \sim 10 using 1 N NaOH, extracted with ethyl acetate (3 \times 150 mL), concentrated in vacuo, and purified by column chromatography to give the desired products as white solids.

3-(Aminomethyl)-4-phenyl-1,2,5-oxadiazole 2-Oxide (**8a**). Synthesized following the general procedure with the following quantities: **2a** (70 mg, 0.32 mmol), $P(Ph)_3$ (1.33 g, 5.06 mmol), 35% NH_4OH (1.26 mL), and DMF (8.4 mL, 0.038 M reaction concentration) yielded **8a** (78 mg, 33.3%). 1H NMR ($CDCl_3$, 400 MHz): δ 7.66–7.61 (m, 3H), 7.57–7.52 (m, 2H), 3.94 (s, 2H), 1.60 (bs, 2H). ^{13}C NMR ($CDCl_3$, 100 MHz): 156.54, 131.54, 129.51, 127.64, 125.79, 111.78, 42.82.

3-(Aminomethyl)-4-(4-methoxyphenyl)-1,2,5-oxadiazole 2-Oxide (**8b**). Synthesized following the general procedure with the following quantities: **2b** (284 mg, 1.48 mmol), $P(Ph)_3$ (6.13 g, 23.4 mmol), 35% $NH_4OH(aq)$ (6.0 mL), and DMF (32 mL) yielded **8b** (98 mg, 38.5%). 1H NMR ($CDCl_3$, 400 MHz): δ 7.71–7.68 (d, 2H), 7.09–7.05 (d, 2H), 4.10 (s, 2H). ^{13}C NMR ($CDCl_3$, 100 MHz): 161.10, 155.15, 129.19, 118.11, 114.54, 112.71, 48.52.

General Coupling Procedure. The appropriate carboxylic acid (1 equiv) was dissolved in anhydrous CH_2Cl_2 and brought to 0 °C under argon. DMAP (0.5 equiv) and EDCI (1.1 equiv) were added and the suspension stirred for 15 min at 0 °C. The furoxan amine (1.0 equiv) dissolved in anhydrous CH_2Cl_2 (5 mL) was added slowly at 0 °C. The reaction was allowed to warm to rt and stirred overnight. The mixture was quenched w/1 N HCl, diluted with ice water, and extracted with CH_2Cl_2 (3 \times 50 mL). Combined organic layers were washed with brine (2 \times 25 mL), dried over Na_2SO_4 , and concentrated to give crude yellow oil. The residual oil purified by column chromatography to give the corresponding furoxan peptidomimetics.

(*R*)-3-((4-Methyl-2-(phenylsulfonamido)pentanamido)methyl)-4-phenyl-1,2,5-oxadiazole 2-Oxide (**9a**). Synthesized using the general procedure with the following values: **8a** (111 mg, 0.58 mmol), EDCI (130 mg, 0.69 mmol), DMAP (40 mg, 0.3 mmol), and peptidomimetic acid (190 mg, 0.69 mmol) afforded **9a** as a white solid (244 mg, 95.4%). 1H NMR ($CDCl_3$, 400 MHz): δ 7.85–7.79 (m, 4H), 7.59–7.42 (m, 6H), 6.85–6.83 (t, 1H), 5.154–5.135 (d, 1H), 4.53–4.30 (m, 2H), 3.75–3.71 (m, 1H), 1.59–1.52 (m, 1H), 1.45–1.41 (m, 2H), 0.851–0.834 (d, 3H), 0.703–0.687 (3H). ^{13}C NMR ($CDCl_3$, 100 MHz): 171.91, 156.24, 139.00, 133.17, 131.30, 129.37, 129.05, 127.93,

127.24, 125.80, 112.94, 55.39, 42.25, 32.28, 24.27, 22.88, 20.98. ESI-HRMS (m/z): $[M + H]^+$ calcd for $C_{21}H_{24}N_4O_5S$, 445.1491; obsd, 445.1556; $[M - H]^+$ calcd for $C_{21}H_{24}N_4O_5S$, 443.1443; obsd, 443.1447. Analytical HPLC (instrument 2): purity = 98.5%, t_R = 25.2 min.

(*R*)-4-(4-Methoxyphenyl)-3-((4-methyl-2-(phenylsulfonamido)pentanamido)methyl)-1,2,5-oxadiazole 2-Oxide (**9b**). Synthesized using the general procedure with the following values: **8b** (40 mg, 0.21 mmol), EDCI (48 mg, 0.25 mmol), DMAP (20 mg, 0.25 mmol), and peptidomimetic acid (68 mg, 0.25 mmol) afforded **9b** as a white solid (75 mg, 80.7%). 1H NMR (MeOD- d_4 , 400 MHz): δ 7.81–7.80 (m, 2H), 7.70–7.68 (d, 2H, J = 9.2 Hz), 7.57–7.46 (m, 3H), 7.09–7.07 (d, 2H, J = 9.2 Hz), 5.5 (s, 1H), 4.28–4.05 (q, 2H), 3.68–3.65 (q, 1H), 1.49–1.41 (m, 1H), 1.29–1.21 (m, 1H), 1.08–1.03 (m, 1H), 0.78–0.76 (d, 3H, J = 6.8 Hz), 0.66–0.65 (d, 3H, J = 6.8 Hz). ^{13}C NMR (MeOD- d_4 , 100 MHz): 171.91, 161.97, 155.83, 150.45, 145.07, 138.95, 133.20, 130.85, 129.42, 129.04, 128.78, 127.23, 117.96, 114.84, 112.85, 55.39, 42.25, 32.28, 24.27, 22.88, 20.98. ESI-HRMS (m/z): $[M + H]^+$ calcd for $C_{22}H_{26}N_4O_6S$, 475.1597; obsd, 475.1650; $[M - H]^+$ calcd for $C_{22}H_{26}N_4O_6S$, 473.1549; obsd, 473.1530. Analytical HPLC (instrument 2): purity = 99.5%, t_R = 25.7 min.

(*R*)-4-Methyl-N-((4-phenyl-1,2,5-oxadiazol-3-yl)methyl)-2-(phenylsulfonamido)pentanamide (**10**). Activated zinc dust (40 mg, 0.5 mmol) was added to a solution of **9a** (120 mg, 0.27 mmol) in anhydrous MeOH (5 mL) and the reaction stirred for 15 min. Ammonium formate (50 mg, 0.8 mmol) was then added in one portion and the reaction was refluxed at 60 °C for 8 h. The reaction mixture was then cooled to room temperature, filtered through Celite, concentrated, and purified by column chromatography to give the desired product as a white solid (15 mg, 13.0%). 1H NMR (CDCl₃, 400 MHz): δ 7.85–7.85 (d, 2H, J = 1.6 Hz), 7.69–7.66 (m, 2H), 7.57–7.44 (m, 6H), 6.76–6.75 (t, 1H), 4.73–4.60 (m, 2H), 3.76–3.72 (m, 1H), 1.51–1.46 (m, 2H), 1.39–1.36 (m, 1H), 0.84–0.81 (d, 3H, J = 6.8 Hz), 0.68–0.63 (d, 3H, J = 6.8 Hz). ^{13}C NMR (CDCl₃, 100 MHz): 171.55, 153.05, 150.29, 139.05, 133.15, 130.85, 129.33, 129.19, 128.14, 127.27, 125.03, 55.43, 41.98, 34.11, 24.26, 22.86, 21.01. ESI-HRMS (m/z): $[M + H]^+$ calcd for $C_{21}H_{24}N_4O_4S$, 429.1542; obsd, 429.1573. Analytical HPLC (instrument 1): purity = 95.2%, t_R = 19.9 min.

■ ASSOCIATED CONTENT

Supporting Information

Additional experimental methods and adjunct results/discussion. This material is available free of charge via the Internet at <http://pubs.acs.org>.

■ AUTHOR INFORMATION

Corresponding Author

*Phone: 312-355-5282. Fax: 312 996 7107. E-mail: thatcher@uic.edu.

Notes

The authors declare no competing financial interest.

■ ACKNOWLEDGMENTS

The work was supported by NIH grant U01 AG028713.

■ ABBREVIATIONS USED

sGC, soluble guanylyl cyclase; cGKs, cGMP-dependent protein kinases; CREB, cyclic-AMP response element binding protein; LTP, long-term potentiation; $A\beta$, amyloid β ; AD, Alzheimer's disease; BDNF, brain derived neurotrophic growth factor; OGD, oxygen glucose deprivation; MTT, 3-(4,5-dimethylthiazol-2-yl)-2,5-diphenyltetrazolium bromide; GSNO, *S*-nitrosoglutathione; DTNB, 5,5'-dithiobis-2-nitrobenzoic acid; ODQ, 1*H*-[1,2,4]-oxadiazolo[4,3-*a*]quinoxalin-1-one; NO_x, a nitrogen oxide (including NO, NO₂⁻, and NO₃⁻)

■ REFERENCES

- (1) Ghosh, P.; Ternai, B.; Whitehouse, M. Benzofuroxans and benzofuroxans: biochemical and pharmacological properties. *Med. Res. Rev.* **1981**, *1*, 159–187.
- (2) Stuart, K. L. Furazans. *Heterocycles* **1975**, *3*, 651–690.
- (3) Cerecetto, H.; Gonzalez, M. Benzofuroxan and furoxan. Chemistry and biology. *Top. Heterocycl. Chem.* **2007**, *10*, 265–308.
- (4) Medana, C.; Ermondi, G.; Fruttero, R.; Di Stilo, A.; Ferretti, C.; Gasco, A. Furoxans as nitric oxide donors. 4-Phenyl-3-furoxancarbonitrile: thiol-mediated nitric oxide release and biological evaluation. *J. Med. Chem.* **1994**, *37*, 4412–4416.
- (5) Ghosh, P. B.; Whitehouse, M. W. Potential antileukemic and immunosuppressive drugs. Preparation and in vitro pharmacological activity of some benzo-2,1,3-oxadiazoles (benzofuroxans) and their *N*-oxides (benzofuroxans). *J. Med. Chem.* **1968**, *11*, 305–311.
- (6) Whitehouse, M. W.; Ghosh, P. B. 4-Nitrobenzofuroxans and 4-nitrobenzofuroxans: a new class of thiol-neutralising agents and potent inhibitors of nucleic acid synthesis in leucocytes. *Biochem. Pharmacol.* **1968**, *17*, 158–161.
- (7) Ferioli, R.; Fazzini, A.; Folco, G. C.; Fruttero, R.; Calvino, R.; Gasco, A.; Bongrani, S.; Civelli, M. NO-mimetic furoxans: arylsulfanyl furoxans and related compounds. *Pharm. Res.* **1993**, *28*, 203–212.
- (8) Boschi, D.; Di Stilo, A.; Cena, C.; Lolli, M.; Fruttero, R.; Gasco, A. Studies on agents with mixed NO-dependent vasodilating and beta-blocking activities. *Pharm. Res.* **1997**, *14*, 1750–1758.
- (9) Boschi, D.; Tron, G. C.; Di Stilo, A.; Fruttero, R.; Gasco, A.; Poggesi, E.; Motta, G.; Leonardi, A. New potential uroselective NO-donor alpha1-antagonists. *J. Med. Chem.* **2003**, *46*, 3762–3765.
- (10) Buonsanti, M. F.; Bertinaria, M.; Di Stilo, A.; Cena, C.; Fruttero, R.; Gasco, A. Nitric Oxide Donor beta 2-Agonists: Furoxan Derivatives Containing the Fenoterol Moiety and Related Furazans. *J. Med. Chem.* **2007**, *50*, S003–S011.
- (11) Cena, C.; Boschi, D.; Tron, G. C.; Chegaev, K.; Lazzarato, L.; Di Stilo, A.; Aragno, M.; Fruttero, R.; Gasco, A. Development of a new class of potential antiatherosclerosis agents: NO-donor antioxidants. *Bioorg. Med. Chem. Lett.* **2004**, *14*, S971–S974.
- (12) Cena, C.; Lolli, M. L.; Lazzarato, L.; Guaita, E.; Morini, G.; Coruzzi, G.; McElroy, S. P.; Megson, I. L.; Fruttero, R.; Gasco, A. Antiinflammatory, gastrosparring, and antiplatelet properties of new NO-donor esters of aspirin. *J. Med. Chem.* **2003**, *46*, 747–754.
- (13) Chegaev, K.; Cena, C.; Giorgis, M.; Rolando, B.; Tosco, P.; Bertinaria, M.; Fruttero, R.; Carrupt, P.-A.; Gasco, A. Edaravone Derivatives Containing NO-Donor Functions. *J. Med. Chem.* **2009**, *52*, S74–S78.
- (14) Sorba, G.; Galli, U.; Cena, C.; Fruttero, R.; Gasco, A.; Morini, G.; Adami, M.; Coruzzi, G.; Brenciaglia, M. I.; Dubini, F. A new furoxan NO-donor rabepazole derivative and related compounds. *ChemBioChem* **2003**, *4*, 899–903.
- (15) Tosco, P.; Bertinaria, M.; Di Stilo, A.; Cena, C.; Sorba, G.; Fruttero, R.; Gasco, A. Furoxan analogues of the histamine H3-receptor antagonist imoproxifan and related furazan derivatives. *Bioorg. Med. Chem.* **2005**, *13*, 4750–4759.
- (16) Velazquez, C.; Rao, P. N.; McDonald, R.; Knaus, E. E. Synthesis and biological evaluation of 3,4-diphenyl-1,2,5-oxadiazole-2-oxides and 3,4-diphenyl-1,2,5-oxadiazoles as potential hybrid COX-2 inhibitor/nitric oxide donor agents. *Bioorg. Med. Chem.* **2005**, *13*, 2749–2757.
- (17) Buonsanti, M. F.; Bertinaria, M.; Stilo, A. D.; Cena, C.; Fruttero, R.; Gasco, A. Nitric oxide donor beta2-agonists: furoxan derivatives containing the fenoterol moiety and related furazans. *J. Med. Chem.* **2007**, *50*, S003–S011.
- (18) Boiani, L.; Aguirre, G.; Gonzalez, M.; Cerecetto, H.; Chidichimo, A.; Cazzulo, J. J.; Bertinaria, M.; Guglielmo, S. Furoxan, alkyl nitrate-derivatives and related compounds as anti-trypanosomatid agents: mechanism of action studies. *Bioorg. Med. Chem.* **2008**, *16*, 7900–7907.
- (19) Boiani, M.; Cerecetto, H.; Gonzalez, M.; Risso, M.; Olea-Azar, C.; Piro, O. E.; Castellano, E. E.; Lopez de Cerain, A.; Ezpeleta, O.; Monge-Vega, A. 1,2,5-Oxadiazole *N*-oxide derivatives as potential anti-

cancer agents: synthesis and biological evaluation. Part IV. *Eur. J. Med. Chem.* **2001**, *36*, 771–782.

(20) Thatcher, G. R. J.; Nicolescu, A. C.; Bennett, B. M.; Toader, V. Nitrates and NO release: contemporary aspects in biological and medicinal chemistry. *Free Radical Biol. Med.* **2004**, *37*, 1122–1143.

(21) Thatcher, G. R. J.; Bennett, B. M.; Reynolds, J. N. NO chimeras as therapeutic agents in Alzheimer's disease. *Curr. Alzheimer Res.* **2006**, *3*, 237–245.

(22) Zhuo, M.; Hu, Y.; Schultz, C.; Kandel, E. R.; Hawkins, R. D. Role of guanylyl cyclase and cGMP-dependent protein kinase in long-term potentiation. *Nature* **1994**, *368*, 635–639.

(23) Lu, Y. F.; Kandel, E. R.; Hawkins, R. D. Nitric oxide signaling contributes to late-phase LTP and CREB phosphorylation in the hippocampus. *J. Neurosci.* **1999**, *19*, 10250–10261.

(24) Bon, C. L.; Garthwaite, J. On the role of nitric oxide in hippocampal long-term potentiation. *J. Neurosci.* **2003**, *23*, 1941–1948.

(25) Haley, J. E.; Wilcox, G. L.; Chapman, P. F. The role of nitric oxide in hippocampal long-term potentiation. *Neuron* **1992**, *8*, 211–216.

(26) Arancio, O.; Kiebler, M.; Lee, C. J.; Lev-Ram, V.; Tsien, R. Y.; Kandel, E. R.; Hawkins, R. D. Nitric oxide acts directly in the presynaptic neuron to produce long-term potentiation in cultured hippocampal neurons. *Cell* **1996**, *87*, 1025–1035.

(27) Mohr, S.; Zech, B.; Lapetina, E. G.; Brune, B. Inhibition of caspase-3 by S-nitrosation and oxidation caused by nitric oxide. *Biochem. Biophys. Res. Commun.* **1997**, *238*, 387–391.

(28) Puzzo, D.; Vitolo, O.; Trinchese, F.; Jacob, J. P.; Palmeri, A.; Arancio, O. Amyloid-beta peptide inhibits activation of the nitric oxide/cGMP/cAMP-responsive element-binding protein pathway during hippocampal synaptic plasticity. *J. Neurosci.* **2005**, *25*, 6887–6897.

(29) Lipton, S. A.; Choi, Y. B.; Pan, Z. H.; Lei, S. Z.; Chen, H. S.; Sucher, N. J.; Loscalzo, J.; Singel, D. J.; Stamler, J. S. A redox-based mechanism for the neuroprotective and neurodestructive effects of nitric oxide and related nitroso-compounds. *Nature* **1993**, *364*, 626–632.

(30) Thatcher, G. R. J. An introduction to NO-related therapeutic agents. *Curr. Top. Med. Chem.* **2005**, *5*, 597–601.

(31) Smith, S.; Dringenberg, H. C.; Bennett, B. M.; Thatcher, G. R. J.; Reynolds, J. N. A novel nitrate ester reverses the cognitive impairment caused by scopolamine in the Morris water maze. *Neuroreport* **2000**, *11*, 3883–3886.

(32) Reynolds, J. N.; Bennett, B. M.; Boegman, R. J.; Jhamandas, K.; Ratz, J. D.; Zavorin, S. I.; Scutaru, D.; Dumitrascu, A.; Thatcher, G. R. J. Neuroprotection against ischemic brain injury conferred by a novel nitrate ester. *Bioorg. Med. Chem. Lett.* **2002**, *12*, 2863–2866.

(33) Vitolo, O. V.; Sant'Angelo, A.; Costanzo, V.; Battaglia, F.; Arancio, O.; Shelanski, M. Amyloid beta peptide inhibition of the PKA/CREB pathway and long-term potentiation: reversibility by drugs that enhance cAMP signaling. *Proc. Natl. Acad. Sci. U.S.A.* **2002**, *99*, 13217–13221.

(34) Puzzo, D.; Staniszewski, A.; Deng, S. X.; Privitera, L.; Leznik, E.; Liu, S.; Zhang, H.; Feng, Y.; Palmeri, A.; Landry, D. W.; Arancio, O. Phosphodiesterase 5 inhibition improves synaptic function, memory, and amyloid-beta load in an Alzheimer's disease mouse model. *J. Neurosci.* **2009**, *29*, 8075–8086.

(35) Blurton-Jones, M.; Kitazawa, M.; Martinez-Coria, H.; Castello, N. A.; Müller, F.-J.; Loring, J. F.; Yamasaki, T. R.; Poon, W. W.; Green, K. N.; LaFerla, F. M. Neural stem cells improve cognition via BDNF in a transgenic model of Alzheimer disease. *Proc. Natl. Acad. Sci. U.S.A.* **2009**, *106*, 13594–13599.

(36) Peng, S.; Wu, J.; Mufson, E. J.; Fahnestock, M. Precursor form of brain-derived neurotrophic factor and mature brain-derived neurotrophic factor are decreased in the pre-clinical stages of Alzheimer's disease. *J. Neurochem.* **2005**, *93*, 1412–1421.

(37) Puzzo, D.; Palmeri, A.; Arancio, O. Involvement of the nitric oxide pathway in synaptic dysfunction following amyloid elevation in Alzheimer's disease. *Rev. Neurosci.* **2006**, *17*, 497–523.

(38) Hook, V.; Kindy, M.; Hook, G. Cysteine protease inhibitors effectively reduce in vivo levels of brain beta-amyloid related to Alzheimer's disease. *Biol. Chem.* **2007**, *388*, 247–252.

(39) Trinchese, F.; Fa, M.; Liu, S.; Zhang, H.; Hidalgo, A.; Schmidt, S. D.; Yamaguchi, H.; Yoshii, N.; Mathews, P. M.; Nixon, R. A.; Arancio, O. Inhibition of calpains improves memory and synaptic transmission in a mouse model of Alzheimer disease. *J. Clin. Invest.* **2008**, *118*, 2796–2807.

(40) Balicki, R.; Cybulski, M.; Maciejewski, G. An Efficient Deoxygenation of Heteroaromatic N-Oxides Using Zinc Dust/Ammonium Formate Reagent System. *Synth. Commun.* **2003**, *33*, 4137–4141.

(41) Medana, C.; Di Stilo, A.; Visentin, S.; Fruttero, R.; Gasco, A.; Ghigo, D.; Bosia, A. NO donor and biological properties of different benzofuroxans. *Pharm. Res.* **1999**, *16*, 956–960.

(42) Sako, M.; Oda, S.; Ohara, S.; Hirota, K.; Maki, Y. *J. Org. Chem.* **1998**, *63*, 6947.

(43) Feelisch, M.; Schönafingeri, K.; Noack, H. Thiol-mediated generation of nitric oxide accounts for the vasodilator action of furoxans. *Biochem. Pharmacol.* **1992**, *44*, 1149–1157.

(44) Sorba, G.; Medana, C.; Fruttero, R.; Cena, C.; Di Stilo, A.; Galli, U.; Gasco, A. Water soluble furoxan derivatives as NO prodrugs. *J. Med. Chem.* **1997**, *40*, 463–469.

(45) Ferioli, R.; Folco, G. C.; Ferretti, C.; Gasco, A. M.; Medana, C.; Fruttero, R.; Civelli, M.; Gasco, A. A new class of furoxan derivatives as NO donors: mechanism of action and biological activity. *Br. J. Pharmacol.* **1995**, *114*, 816–820.

(46) Rai, G.; Sayed, A. A.; Lea, W. A.; Luecke, H. F.; Chakrapani, H.; Prast-Nielsen, S.; Jadhav, A.; Leister, W.; Shen, M.; Inglese, J.; Austin, C. P.; Keefer, L.; Arner, E. S.; Simeonov, A.; Maloney, D. J.; Williams, D. L.; Thomas, C. J. Structure mechanism insights and the role of nitric oxide donation guide the development of oxadiazole-2-oxides as therapeutic agents against schistosomiasis. *J. Med. Chem.* **2009**, *52*, 6474–6483.

(47) Boiani, M.; Cerecetto, H.; González, M.; Risso, M.; Olea-Azar, C.; Piro, O. E.; Castellano, E. E.; López de Ceráin, A.; Ezpeleta, O.; Monge-Vega, A. 1,2,5-Oxadiazole N-oxide derivatives as potential anti-cancer agents: synthesis and biological evaluation. Part IV. *Eur. J. Med. Chem.* **2001**, *36*, 771–782.

(48) Melino, G.; Bernassola, F.; Knight, R. A.; Corasaniti, M. T.; Nistic, G.; Finazzi-Agr, A. S-nitrosylation regulates apoptosis. *Nature* **1997**, *388*, 432–433.

(49) Ascenzi, P.; Bocedi, A.; Gentile, M.; Visca, P.; Gradoni, L. Inactivation of parasite cysteine proteinases by the NO-donor 4-(phenylsulfonyl)-3-((2-(dimethylamino)ethyl)thio)-furoxan oxalate. *Biochim. Biophys. Acta* **2004**, *1703*, 69–77.

(50) Ascenzi, P.; Salvati, L.; Bolognesi, M.; Colasanti, M.; Polticelli, F.; Venturini, G. Inhibition of cysteine protease activity by NO-donors. *Curr. Protein Pept. Sci.* **2001**, *2*, 137–153.

(51) Loo, D. T.; Rillema, J. R.; Jennie, P. M.; David, B. Measurement of Cell Death. *Methods in Cell Biology*; Academic Press: New York, 1998; Vol. 57, Chapter 14, pp 251–264.

(52) Goldberg, M. P.; Strasser, U.; Dugan, L. L. Techniques for assessing neuroprotective drugs in vitro. *Int. Rev. Neurobiol.* **1997**, *40*, 69–93.

(53) Lee, K. S.; Frank, S.; Vanderklish, P.; Arai, A.; Lynch, G. Inhibition of proteolysis protects hippocampal neurons from ischemia. *Proc. Natl. Acad. Sci. U.S.A.* **1991**, *88*, 7233–7237.

(54) Rami, A.; Kriegstein, J. Protective effects of calpain inhibitors against neuronal damage caused by cytotoxic hypoxia in vitro and ischemia in vivo. *Brain Res.* **1993**, *609*, 67–70.

(55) Komatsu, K.; Inazuki, K.; Hosoya, J.; Satoh, S. Beneficial effect of new thiol protease inhibitors, epoxide derivatives, on dystrophic mice. *Exp. Neurol.* **1986**, *91*, 23–29.

(56) Kandel, E. R. The molecular biology of memory storage: a dialogue between genes and synapses. *Science* **2001**, *294*, 1030–1038.

(57) Lambert, M. P.; Barlow, A. K.; Chromy, B. A.; Edwards, C.; Freed, R.; Liosatos, M.; Morgan, T. E.; Rozovsky, I.; Trommer, B.; Viola, K. L.; Wals, P.; Zhang, C.; Finch, C. E.; Krafft, G. A.; Klein, W.

L. Diffusible, nonfibrillar ligands derived from Abeta1–42 are potent central nervous system neurotoxins. *Proc. Natl. Acad. Sci. U.S.A.* **1998**, *95*, 6448–6453.

(58) Arancio, O.; Kiebler, M.; Lee, C. J.; Lev-Ram, V.; Tsien, R. Y.; Kandel, E. R.; Hawkins, R. D. Nitric Oxide Acts Directly in the Presynaptic Neuron to Produce Long-Term Potentiation in Cultured Hippocampal Neurons. *Cell* **1996**, *87*, 1025–1035.

(59) Brewer, G. J.; Torricelli, J. R.; Evege, E. K.; Price, P. J. Optimized survival of hippocampal neurons in B27-supplemented Neurobasal, a new serum-free medium combination. *J. Neurosci. Res.* **1993**, *35*, 567–576.